Available online at www.sciencedirect.com
ScienceDirect
Trans. Nonferrous Met. Soc. China 26(2016) 1025−1031
Transactions of Nonferrous Metals Society of China
www.tnmsc.cn

Microstructure and mechanical properties of Fe-doped NiAl−28Cr−6Mo eutectic alloys

A. GUNGOR, H. DEMIRTAS

Metallurgical and Materials Engineering Department, Engineering Faculty, Karabuk University, Karabuk 78050, Turkey

Received 20 May 2015; accepted 24 July 2015

Abstract: Room temperature and high temperature microstructural and mechanical properties of arc melted NiAl−28Cr−6Mo eutectic alloys doped with 0.1% Fe, 0.2% Fe and 0.5% Fe (mole fraction) were investigated. The homogenization heat treatment of the alloys was conducted at 1300 °C in Ar atmosphere. Microscopic analyses, hardness measurements, XRD measurements and compression tests were used to characterize the alloys. As-cast and homogenized alloys exhibit fine cellular eutectic structures with coarse intercellular eutectic structure. The increase in the content of Fe results in coarsening eutectic layers and the decrease in eutectic cells. All alloys have very high compressive stress and strain at room temperature. The addition of Fe has small negative impact on the strength and ductility of the alloys at room temperature. However, the addition of Fe increases the high temperature strength of the alloy. High temperature XRD patterns show that peaks shift to lower Bragg angles. This indicates that the lattice parameter of the alloys increases.

Key words: aluminium alloy; microalloying; solid-solution hardening; brittleness; ductility; microstructure; mechanical properties

1 Introduction

Ordered intermetallic materials have taken considerable attention for high temperature structural applications in last two decades. Among the intermetallics, NiAl intermetallic compound with *B*2 crystal structure has excellent properties including high melting point, low density, good thermal conductivity and excellent oxidation resistance up to 1300 °C [1–5]. Such attractive properties make NiAl candidate for high temperature structural applications. However, low ductility and fracture toughness at room temperature and poor elevated temperature strength of the NiAl limit its commercial applications significantly [6,7]. Some strengthening and toughening approaches such as alloying, second-phase strengthening and single crystal preparation have been proposed to overcome the drawbacks of NiAl [8−12]. Previous studies on NiAl revealed that the addition of refractory metals like Cr, Mo, V and Ta, can improve the room temperature toughness and elevated temperature strength of NiAl simultaneously [13−15]. WALTER and CLINE [13] showed that directionally solidified NiAl−Cr eutectic alloy strengthened by the Cr fiber had better toughness and creep strength than NiAl alloy. In addition, CLINE et al [16,17] showed that adding Mo to the NiAl–Cr eutectic alloy would lead to a change of microstructure from Cr fibers to Cr(Mo) lamels.

Among the eutectic alloys, NiAl–28Cr–6Mo alloy is very attractive due to its good room temperature ductility and fracture toughness as well as good high temperature strength [18]. The low and high temperature mechanical properties of NiAl−28Cr−6Mo eutectic alloy can be further improved with microalloying. Therefore, it is of interest to investigate the room and high temperature microstructure and mechanical properties of the Fe-containing NiAl−Cr(Mo) eutectic alloys since there are not enough studies on the arc melted and microalloyed eutectic alloys. Here, we present low and high temperature microstructure and mechanical properties of arc melted (66−*x*)NiAl−28Cr−6Mo−*x*Fe eutectic alloys.

2 Experimental

(66−*x*)NiAl−28Cr−6Mo−*x*Fe eutectic alloys with nominal compositions of *x*=0.1, 0.2 and 0.5 (mole fraction, %) were prepared by vacuum arc melting using Edmund Buhler vacuum arc melter. The purities of metal powders used in this work are 99.9% Ni, 99.9% Al, 99.99% Cr, 99.95% Mo and 99.98% Fe. Before melting

Corresponding author: A. GUNGOR; E-mail: agungor@karabuk.edu.tr
DOI: 10.1016/S1003-6326(16)64199-7

the alloys, the mixture of metal powders was cold-pressed. All arc melted buttons were turned over and remelted at least four times to get homogeneous specimens. In addition, homogenization heat treatment of the alloys was performed at 1300 °C for 24 h in Ar atmosphere (40 L/h). After that, all alloys were furnace-cooled. Before the homogenization heat treatment, the atmosphere of the furnace was purged three times by filling high purity Ar and then vacuuming to 6.5 Pa. Since the mass loss for each sample was less than 0.5%, the alloy compositions were considered to be equal to their nominal compositions.

Wire electro-discharged machine (EDM) was used to get specimens for microstructure analyses and compression tests. For microstructure analyses, specimens were cut along the longitudinal and transverse directions of arc melted buttons. The sections were mechanically polished and then etched in a 5% nital solution. The microstructure of the alloys and chemical composition of the phases were characterized using scanning electron microscope (SEM, Carl Zeiss Ultra Plus Gemini FESEM) with attached energy-dispersive X-ray spectrometer (EDS). The room temperature and high temperature (1000 °C) X-ray diffraction (XRD, Rigaku Ultra IV diffractometer) measurements were conducted at a rate of 4 (°)/min between 25°−85° using 40 kV and 30 mA. The Brinell hardness (HB 2.5, HB 31.25, HB 10) of the homogenized alloys was determined by applying 31.25 kg load on 2.5 mm steel ball for 10 s on a Qness/Q250M hardness device. For each alloy, the average hardness of the alloys was obtained from three hardness measurements. The compression tests were performed after homogenization heat treatment. In compression tests, cylindrical specimens with 3 mm in diameter and 5 mm in height were used. The room temperature compression tests were performed at a strain rate of 5×10^{-4} s^{-1} on a Zwick/Roell Z600 static/dynamic test machine. The high temperature (1000 °C) compression tests were performed at a strain rate of 5×10^{-3} s^{-1} on a Shimadzu AG-IS 250 test machine.

3 Results and discussion

3.1 Microstructural characteristics

The microstructures taken from longitudinal and transverse directions of the specimens are very similar, indicating that rapid cooling of the melt in water cooled copper mold uniformly occurs in all directions. As an example, the microstructures of NiAl−28Cr−6Mo eutectic alloy are given in Fig. 1.

As can be seen from Fig. 1, the as-cast and homogenized alloys have fully cellular eutectic microstructures. In the eutectic cells, dark NiAl and gray

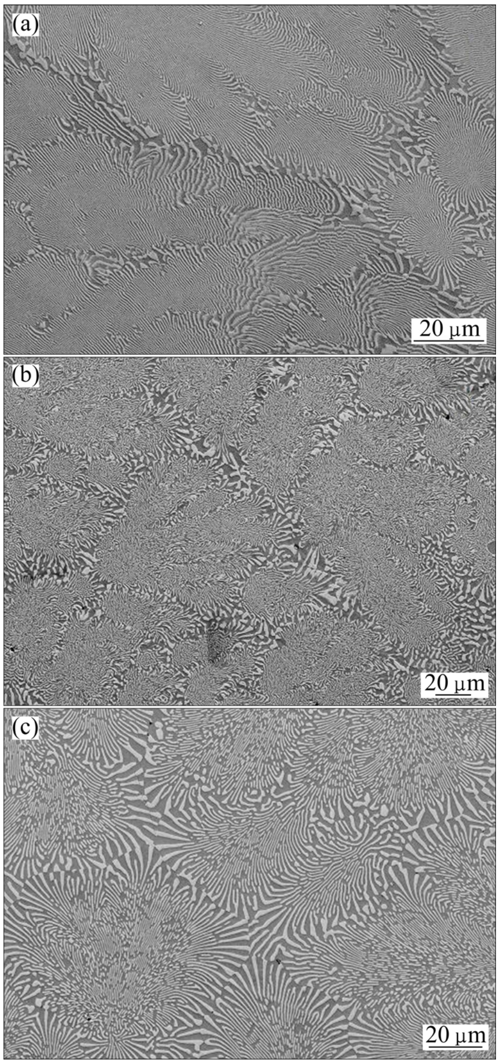

Fig. 1 Microstructures of NiAl−28Cr−6Mo alloy: (a) As-cast structure in traverse direction; (b) Structure after homogenization in traverse direction; (c) Microstructure after homogenization in longitudinal direction

Cr(Mo) lamels radiate from the cell center to the cell boundaries. The interlamellar spacing of the Cr(Mo) and NiAl phases near the cell center is smaller than that near the cell boundary. On the other hand, coarse NiAl and Cr(Mo) phases with irregular morphology exist in the intercellular zone. These microstructures have been respectively observed in Hf-, Ho-, and RE-doped NiAl−Cr(Mo) eutectic, hypoeutectic and hypereutectic alloys prepared by arc melting [19], injection casting [20], and directional solidification [21,22] techniques. Agglomeration and coarsening of eutectic layers occur during homogenization heat treatment. The EDS pattern of homogenized NiAl−28Cr−6Mo alloy is given in Fig. 2. The existence of Ni and Al in the Cr(Mo) phase indicates that small NiAl precipitates in the Cr(Mo) phase, and similarly, Cr(Mo) precipitates exist in the NiAl phase [19,20,23]. The fact that chemical compositions of the Cr(Mo) and NiAl phases in eutectic cell center and in interdendritic region are very similar indicates homogeneity of the alloys.

The typical microstructures of (66−*x*)NiAl−28Cr−6Mo−*x*Fe (*x*=0.1, 0.2 and 0.5, mole fraction, %) alloys before and after homogenization heat treatment are given in Fig. 3. The addition of small amount of Fe to NiAl−28Cr−6Mo has important effects on the microstructure. The intercellular zone gets larger, the Cr(Mo) eutectic plates become coarser and the volume fraction of fine eutectic cells decreases with increasing Fe content. Homogenization heat treatment also results in agglomeration and coarsening of eutectic layers in both Fe-free and Fe-containing alloys.

The distribution of Fe atoms between the phases was determined with EDX point and line analyses. The chemical composition of the phases in 0.2%Fe-containing alloy is shown in Fig. 4. As can be seen from the point and line analyses, Fe partitions both Cr(Mo) and NiAl phases. However, Fe participates into the Cr(Mo) phase a little more than into the NiAl phase as it is seen from Table 1.

Phase analyses of the alloys were performed at room temperature and 1000 °C. The XRD patterns of the homogenized alloys are given in Fig. 5. The room temperature XRD patterns of the alloys show that the alloys have two-phase structure, NiAl and Cr(Mo) phases. These phases have been observed by other researchers in NiAl−Cr(Mo) eutectic alloys containing Ti, Hf, Nb, etc. alloying elements [20,23−25]. At 1000 °C, the peaks slightly shift to lower Bragg angles. This indicates that lattice parameters of the phases increase. The increase in lattice parameters can be due to the increase in the separation of planes at high temperatures.

The room temperature and high temperature XRD patterns of NiAl−Cr(Mo) alloys indicate that crystals have random orientation. The addition of Fe influences the crystal orientation at both temperatures. At room

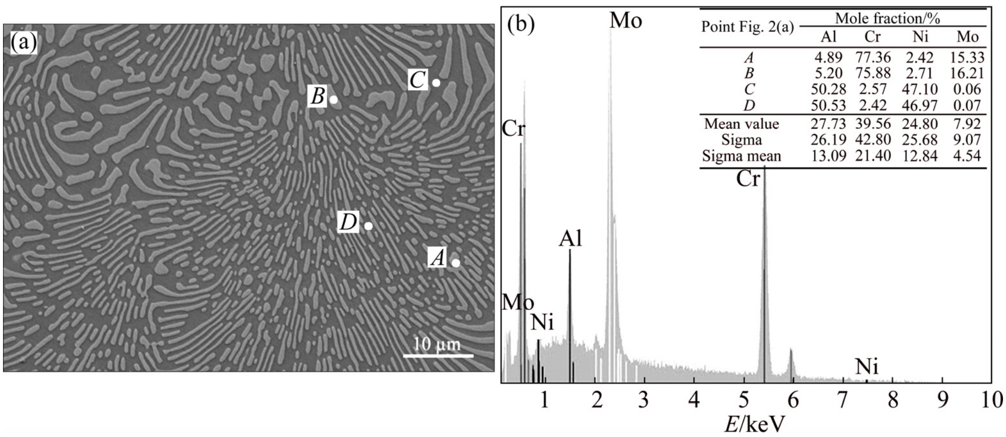

Point Fig. 2(a)	Mole fraction/%			
	Al	Cr	Ni	Mo
A	4.89	77.36	2.42	15.33
B	5.20	75.88	2.71	16.21
C	50.28	2.57	47.10	0.06
D	50.53	2.42	46.97	0.07
Mean value	27.73	39.56	24.80	7.92
Sigma	26.19	42.80	25.68	9.07
Sigma mean	13.09	21.40	12.84	4.54

Fig. 2 EDX point analyses of homogenized NiAl−28Cr−6Mo alloy: (a) Microstructure; (b) EDS pattern

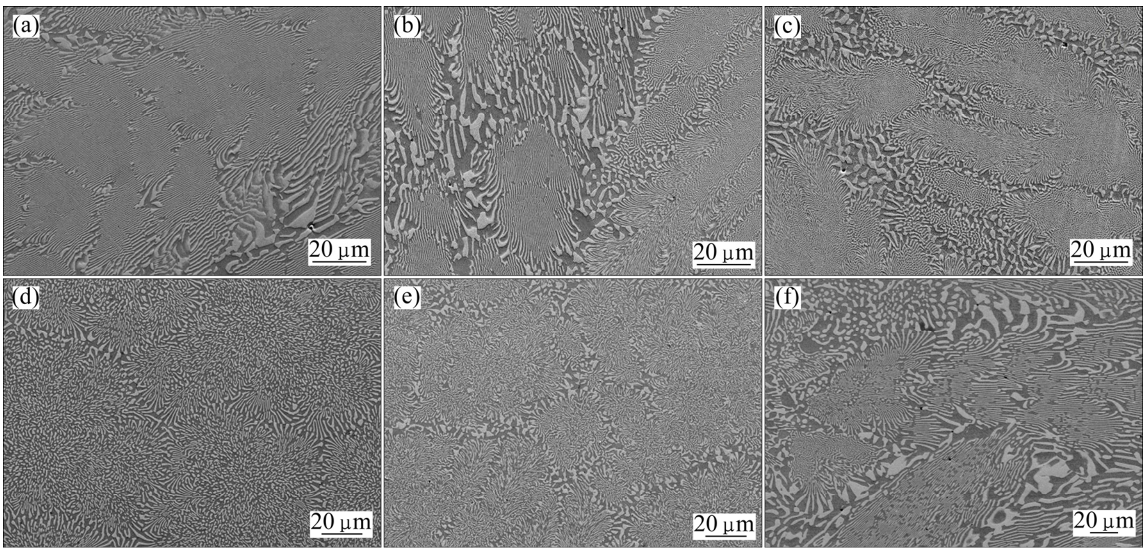

Fig. 3 Microstructures of as-cast (a−c) and homogenized (d−f) (66−*x*)NiAl−28Cr−6Mo−*x*Fe alloys: (a, d) *x*=0.1; (b, e) *x*=0.2; (c, f) *x*=0.5

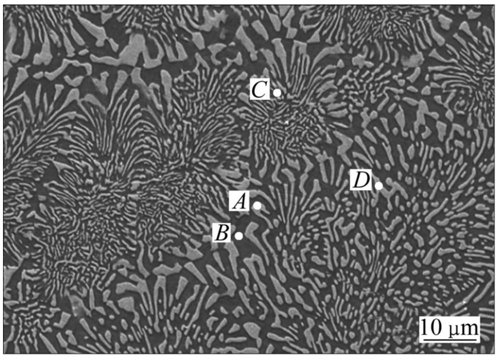

Point	Mole fraction/%				
	Al	Cr	Fe	Ni	Mo
A	5.38	76.12	0.48	2.89	15.13
B	50.04	2.32	0.41	47.13	0.10
C	49.74	2.51	0.34	47.01	0.40
D	4.97	76.61	0.48	3.64	14.29

(a)

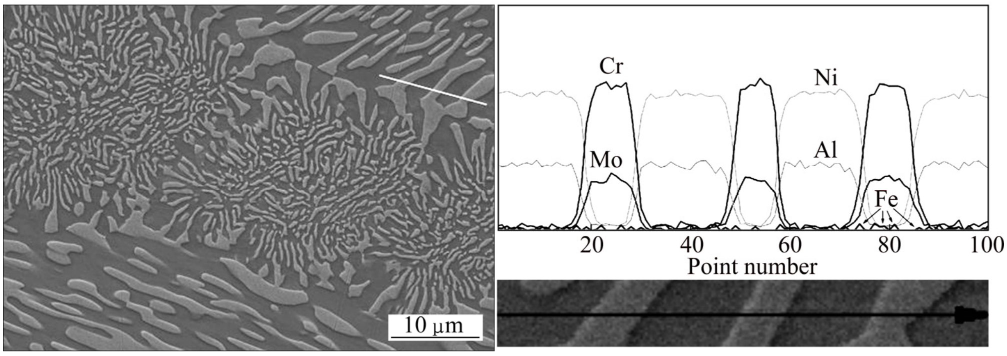

(b)

Fig. 4 EDX point (a) and line (b) analyses of eutectic alloy containing 0.2% Fe

Table 1 Average Fe contents in Cr(Mo) and NiAl phases

Alloy	Average mole fraction of Fe/%	
	Cr(Mo)	NiAl (matrix)
65.9(NiAl)−28Cr−6Mo−0.1Fe	0.42	0.30
65.8(NiAl)−28Cr−6Mo−0.2Fe	0.48	0.38
65.5(NiAl)−28Cr−6Mo−0.5Fe	1.44	0.28

temperature, [110] orientation gets stronger, but [100] and [200] orientations get weaker with the increase of the Fe content. Similar effect is also seen in high temperature XRD patterns. Therefore, Fe addition into NiAl−Cr(Mo) alloy causes a transformation from random orientation to the preferred orientation.

3.2 Hardness properties

Macrohardness test was used instead of microhardness since penetration depth and area are small in microhardness tests due to small applied loads. Therefore, it is not possible to obtain a representative hardness value of the alloys with microhardness measurements. As a result, Brinell hardness of the homogenized alloys was measured by applying 31.25 kg load for 10 s on 2.5 mm steel ball (HB2.5/31.25/10). The hardness values of the alloys are given in Table 2.

As it is seen from the results, the Fe-containing alloys have similar Brinell hardness values. However, the hardness of the NiAl−Cr(Mo) alloy is higher than that of the Fe-containing alloys. The Brinell hardness

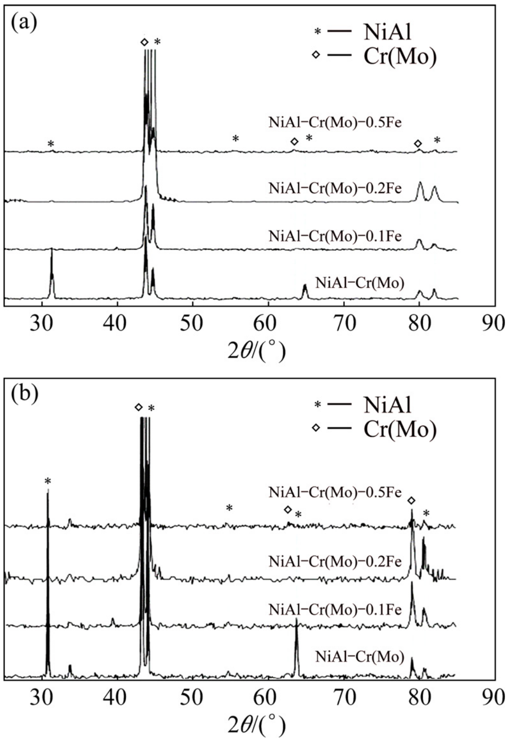

Fig. 5 XRD patterns of alloys: (a) At room temperature; (b) At high temperature of 1000 °C

measurement also provides valuable information on the deformation behavior of the phases, ductility and toughness of the alloys. After Brinell hardness measurements, the surfaces of the alloys are analyzed using SEM in order to determine presence of surface cracks and to understand the behaviour of the Cr(Mo) phase during plastic deformation. The appearances of the indentations are given in Fig. 6.

Table 2 Brinell hardness of eutectic alloys

Alloy	Hardness (HB)			Average hardness (HB)
NiAl−Cr(Mo)	283	270	269	274
NiAl−Cr(Mo)−0.1Fe	259	258	255	257
NiAl−Cr(Mo)−0.2Fe	257	253	248	253
NiAl−Cr(Mo)−0.5Fe	250	262	260	257

Based on the hardness of the alloys, the average diameter of the indentations ranges between 381 μm for NiAl−Cr(Mo) and 400 μm for NiAl−Cr(Mo)−0.2Fe. It has been observed that a significant plastic deformation occurs in Fe-free and 0.2%Fe-containing eutectic alloys without crack formation. However, microcracks form during indentation in 0.1%Fe- and 0.5%Fe-containing eutectic alloys. From microscopic analyses, it can be concluded that the Cr(Mo) phase behaves as barrier to crack propagation because several crack deflection and blunting points have been observed on the crack propagation path. Therefore, the Cr(Mo) phase contributes to the fracture strength of the alloys by absorbing crack energy and slowing down the crack growth rate. Crack formation in the alloys can be explained with the ductility and toughness of the alloys. When a force is applied on the hard metallic phases such as the Cr(Mo) phase, they transfer the applied load to the metallic matrix. The metal matrix such as NiAl solid solution absorbs the energy by going through plastic deformation. If the stress is larger than the fracture strength of the matrix, crack initiation in the matrix occurs. Therefore, it can be said that 0.1%Fe- and 0.5%Fe-containing alloys have lower ductility and toughness than 0.2%Fe-containing alloy. This is related to Fe content and its distribution in the matrix and Cr(Mo) phases. As it is seen in Table 1, the average Fe content of matrix in 0.2%Fe-containing alloy is slightly higher than that of matrices in other Fe-containing alloys. Therefore, the increase in the Fe content of the matrix may be responsible for better ductility and toughness.

3.3 Compressive properties

Mechanical properties of the alloys were determined by compression tests at room temperature and 1000 °C. The stress−strain curves are given in Fig. 7 and mechanical properties of the alloys are given in Table 3. The modulus of elasticity of the alloys in Table 3 is taken from the slope of the stress−strain curves. As it is seen from the room temperature data, all alloys

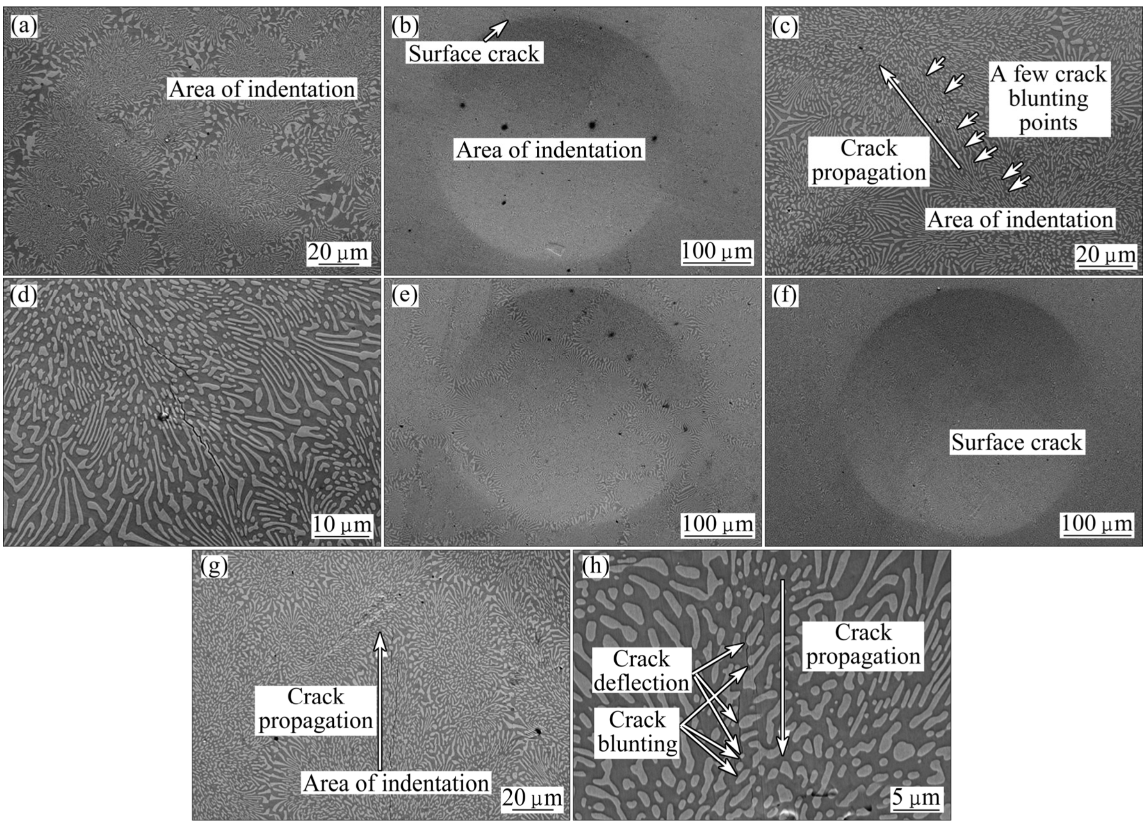

Fig. 6 Crack formation during hardness measurements: (a) NiAl−Cr(Mo); (b−d) NiAl−Cr(Mo)+0.1Fe; (e) NiAl−Cr(Mo)+0.2Fe; (f−h) NiAl−Cr(Mo)+0.5Fe

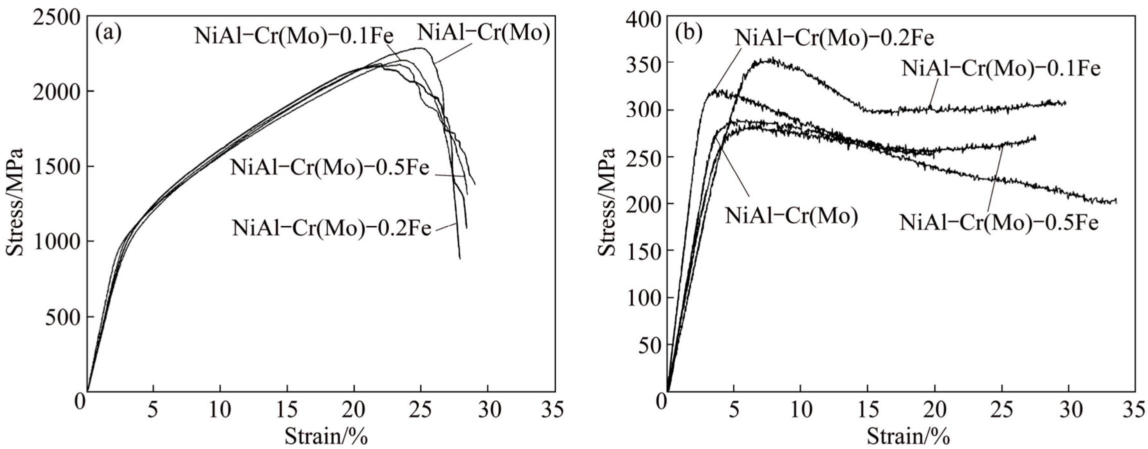

Fig. 7 Compression stress−strain curves of homogenized alloys: (a) At room temperature; (b) At high temperature of 1000 °C

Table 3 Room temperature and high temperature compressive properties of alloys

Alloy	Temperature/°C	E^*/GPa	σ_y/MPa	ε_y/%	σ_u/MPa	ε_u/%
NiAl−Cr(Mo)	RT	36.58	902	2.68	2285	24.33
	1000	8.95	268	3.17	292	5.6
NiAl−Cr(Mo)−0.1Fe	RT	43.82	949.9	2.36	2206.1	23.38
	1000	7.48	261.9	3.71	357	6.80
NiAl−Cr(Mo)−0.2Fe	RT	37.59	966.1	2.77	2165.4	21.35
	1000	13.19	304.4	2.51	322.7	4.10
NiAl−Cr(Mo)−0.5Fe	RT	39.02	995.8	2.76	2180.7	21.26
	1000	7.91	235.6	3.19	287.4	6.50

E: Elastic modulus; σ_y: Yield stress (0.2% offset); ε_y: Yield strain; σ_u: Ultimate compression stress; ε_u: Ultimate compression strain

show very high ductility, yield and ultimate compression stresses. The yield stress of the NiAl−Cr(Mo) eutectic alloy at room temperature increases with the increase of Fe content. On the other hand, the Fe addition lowers the ultimate compression stress and strain of the Fe-free alloy. This can be explained with the degradation of eutectic structure with the increase of Fe content and coarsening of eutectic layers. The increase in the test temperature to 1000 °C results in much lower mechanical properties. 0.1%Fe addition to the NiAl−Cr(Mo) alloy does not have an important effect on the high temperature yield stress. This can be due to the fact that both alloys have very similar structure. However, 0.2%Fe addition increases the yield stress of the NiAl−Cr(Mo) alloy by about 13.5%. Further increase in the Fe content has negative impact on the yield stress. In addition, high temperature ultimate compression stress of Fe-containing alloys increases with the increase of the Fe content except 0.5%Fe. This can be related to the degradation of eutectic cells with the Fe concentration and coarsening of eutectic layers.

4 Conclusions

1) The room temperature and high temperature microstructure and mechanical properties of arc melted NiAl−Cr(Mo) and (66−x)NiAl−28Cr6Mo−xFe (x=0.1, 0.2 and 0.5, mole fraction, %) eutectic alloys were studied. NiAl−Cr(Mo) eutectic alloys have fully lamellar eutectic structure. The Fe addition results in coarser intercellular zone and lower volume fraction of fine eutectic cells. The EDX analyses reveal that Fe partitions both the NiAl and Cr(Mo) phases. The room temperature and high temperature XRD measurements show that all alloys have two-phase structure, NiAl and Cr(Mo).

2) The introduction of the Fe into the base alloy decreases the hardness. Microcrack formation in 0.1%Fe- and 0.5%Fe-containing alloys is observed from the surface analysis of the indentations. It is thought that the Cr(Mo) lamels contribute to the toughness and strength of the alloys with different mechanisms such as absorbing crack energy, crack deflection and blunting.

3) All alloys have very high yield and ultimate stress and strain at room temperature. At a high temperature, mechanical properties of the alloys decrease significantly. Among the alloys, 0.2%Fe-containing alloy has the highest high temperature yield stress. It is thought that the increase in the Fe content in matrix may result in better mechanical properties.

Acknowledgments

The authors gratefully acknowledge the Tubitak for their financial support under Contract No. 213M247.

References

[1] NOEBE R, BOWMAN R, NATHAL M. Physical and mechanical properties of the *B*2 compound NiAl [J]. International Materials Reviews, 1993, 38: 193−232.

[2] MIRACLE D B. Overview No. 104: The physical and mechanical properties of NiAl [J]. Acta Metallurgica et Materialia, 1993, 41: 649−684.

[3] GEORGE E, LIU C. Brittle fracture and grain boundary chemistry of microalloyed NiAl [J]. Journal of Materials Research, 1990, 5: 754−762.

[4] ASSADI H, BARTH M, GREER A, HERLACH D. Kinetics of solidification of intermetallic compounds in the Ni−Al system [J]. Acta Materialia, 1998, 46: 491−500.

[5] DEVRED F, REINHART G, ILES G, van der KLUGT B, ADKINS N, BAKKER J. Synchrotron X-ray microtomography of Raney-type nickel catalysts prepared by gas atomisation: Effect of microstructure on catalytic performance [J]. Catalysis Today, 2011, 163: 13−19.

[6] DAROLIA R. NiAl alloys for high-temperature structural applications [J]. JOM, 1991, 43: 44−49.

[7] GEORGE E, YAMAGUCHI M, KUMAR K, LIU C. Ordered intermetallics [J]. Annual Review of Materials Science, 1994, 24: 409−451.

[8] XIE Y, GUO J, LIANG Y, ZHOU L, YE H. Modification of NiAl−Cr (Mo)−0.15Hf alloy by Sc addition [J]. Intermetallics, 2009, 17: 400−403.

[9] CHEN Y, WANG H. Laser melted TiC reinforced nickel aluminide matrix in situ composites [J]. Journal of Alloys and Compounds, 2005, 391: 49−54.

[10] DAROLIA R, WALSTON W, NOEBE R, GARG A, OLIVER B. Mechanical properties of high purity single crystal NiAl [J]. Intermetallics, 1999, 7: 1195−1202.

[11] LIU E, GAO Y, JIA J, BAI Y, WANG W. Microstructure and mechanical properties of in situ NiAl−Mo_2C nanocomposites prepared by hot-pressing sintering [J]. Materials Science and Engineering A, 2014, 592: 201−206.

[12] FROMMEYER G, RABLBAUER R, SCHÄFER H. Elastic properties of *B*2-ordered NiAl and NiAl−X (Cr, Mo, W) alloys [J]. Intermetallics, 2010, 18: 299−305.

[13] WALTER J L, CLINE H E. The effect of solidification rate on structure and high-temperature strength of the eutectic NiAl−Cr [J]. Metallurgical and Materials Transactions, 1970, 1: 1221−1229.

[14] SHENG L, YANG F, XI T, ZHENG Y, GUO J. Improvement of compressive strength and ductility in NiAl−Cr (Nb)/Dy alloy by rapid solidification and HIP treatment [J]. Intermetallics, 2012, 27: 14−20.

[15] SHENG L, GUO J, ZHOU L, YE H. Microstructure and compressive properties of NiAl−Cr(Mo)−Dy near eutectic alloy prepared by suction casting [J]. Materials Science and Technology, 2010, 26: 164−168.

[16] CLINE H E, WALTER J L. The effect of alloy additions on the rod-plate transition in the eutectic NiAl−Cr [J]. Metallurgical Transactions, 1970, 1: 2907−2917.

[17] CLINE H E, WALTER J L, LIFSHIN E, RUSSELL R. Structures, faults, and the rod-plate transition in eutectics [J]. Metallurgical Transactions, 1971, 2: 189−194.

[18] BEI H, GEORGE E. Microstructures and mechanical properties of a directionally solidified NiAl−Mo eutectic alloy [J]. Acta Materialia, 2005, 53: 69−77.

[19] SHENG L, WANG L, XI T, ZHENG Y, YE H. Microstructure, precipitates and compressive properties of various holmium doped NiAl/Cr (Mo, Hf) eutectic alloys [J]. Materials & Design, 2011, 32: 4810−4817.

[20] SHENG L, FANG Y, XI T, ZHENG Y, GUO J. Microstructure and room temperature mechanical properties of NiAl−Cr(Mo)−(Hf, Dy) hypoeutectic alloy prepared by injection casting [J]. Transactions of Nonferrous Metals Society of China, 2013, 23(3): 983−990.

[21] WANG L, SHEN J, SHANG Z, ZHANG J, DU Y, FU H. Microstructure and mechanical property of directionally solidified NiAl–Cr(Mo)–(Hf, Dy) alloy at different withdrawal rates [J]. Materials Science and Engineering A, 2014, 607: 113−121.

[22] SHANG Z, SHEN J, WANG L, DU Y, XIONG Y, FU H. Investigations on the microstructure and room temperature fracture toughness of directionally solidified NiAl–Cr (Mo) eutectic alloy [J]. Intermetallics, 2015, 57: 25−33.

[23] SHENG L, GUO J, YE H. Microstructure and mechanical properties of NiAl–Cr (Mo)/Nb eutectic alloy prepared by injection-casting [J]. Materials & Design, 2009, 30: 964−969.

[24] HUAI K, GUO J, REN Z, GAO Q, YANG R. Effect of Nb on the microstructure and mechanical properties of cast NiAl−Cr(Mo) eutectic alloy [J]. Journal of Materials Science and Technology, 2006, 22: 164−168.

[25] TANG L Z, ZHANG Z G, LI S S, GONG S K. Mechanical behaviors of NiAl−Cr(Mo)-based near eutectic alloy with Ti, Hf, Nb and W additions [J]. Transactions of Nonferrous Metals Society of China, 2010, 20(2): 212−216.

铁掺杂 NiAl−28Cr−6Mo 共晶合金的显微组织和力学性能

A. GUNGOR, H. DEMIRTAS

Metallurgical and Materials Engineering Department, Engineering Faculty, Karabuk University, Karabuk 78050, Turkey

摘　要：研究掺杂了 0.1%Fe、0.2%Fe 和 0.5%Fe(摩尔分数)的电弧熔炼 NiAl−28Cr−6Mo 共晶合金在室温和高温条件的显微组织和力学性能。合金的均匀化热处理在 Ar 气气氛中于 1300 °C 条件下进行。采用金相分析技术、硬度测试、X 射线衍射分析技术及压缩试验对合金样品进行表征。结果表明，铸态和均匀态合金均呈较细的晶内共晶结构和较粗的晶间共晶结构。Fe 含量的增加导致共晶层粗化及共晶数量减少。在室温条件下所有实验合金均具有很高的压缩应力和应变。Fe 的添加对室温条件下合金的强度和延展性的影响较小；然而，Fe 的添加使合金的高温强度增加。高温条件下，X 射线衍射峰向低 Bragg 角方向移动，这表明 Fe 的添加使合金的晶格常数增大。

关键词：铝合金；微合金化；固−液硬化；脆性；延展性；显微组织；力学性能

(Edited by Wei-ping CHEN)